INTERNATIONAL JOURNAL FOR NUMERICAL METHODS IN FLUIDS
Int. J. Numer. Meth. Fluids 2007; **53**:1495–1507
Published online 27 September 2006 in Wiley InterScience (www.interscience.wiley.com). DOI: 10.1002/fld.1373

Compatibility between finite volumes and finite elements using solutions of shallow water equations for substance transport

Leo Postma[1,*,†] and Jean-Michel Hervouet[2]

[1] *WL|Delft Hydraulics, Rotterdamseweg 185, Netherlands*
[2] *LNHE, National Hydraulics and Environment Laboratory, 6 Quai Watier, 78401 Chatou Cedex, France*

SUMMARY

This paper formulates a finite volume analogue of a finite element schematization of three-dimensional shallow water equations. The resulting finite volume schematization, when applied to the continuity equation, exactly reproduces the set of matrix equations that is obtained by the application of the corresponding finite element schematization to the continuity equation. The procedure allows the consistent and mass conserving coupling of the finite element Telemac model for three-dimensional flow with the finite volume Delft3D-WAQ model for water quality. The work has been carried out as part of a joint development by LNHE and WL|Delft Hydraulics to explore the mutual interaction of their software. Copyright © 2006 John Wiley & Sons, Ltd.

Received 9 March 2006; Revised 12 June 2006; Accepted 13 August 2006

KEY WORDS: finite element method; finite volume method; continuity equation; surface water flow; pollutant transport

1. INTRODUCTION

The finite element method has distinct advantages for the modelling of surface water flow. The flexibility of irregular grids, often composed of triangles, and the accuracy that can be obtained by the different shapes of base functions gives the modeller flexibility. The finite volume method is often the method of choice for water quality modelling because of its natural representation of the law of conservation of mass. The purpose of this joint study is to examine whether it would be feasible to use finite element methods for the modelling of water flow and to use finite volume methods for the modelling of water quality on the thus computed water flow. The method presented here builds on the joint representation of the same set of matrix equations for the representation of the continuity equation to ensure a consistent and mass conserving migration of the flow field

[*] Correspondence to: Leo Postma, WL|Delft Hydraulics, P.O. Box 177, 2600 MH Delft, Netherlands.
[†] E-mail: leo.postma@wldelft.nl

from the hydrodynamic model towards the water quality model. The resulting procedure is simple and easy to implement. A first rudimentary application of this technique took place for Venice Lagoon [1]. Presently a more complete coupling is obtained and the numerical backgrounds are the subject of this contribution. In Section 2 the water levels and velocities as computed with the FE hydrodynamic model are converted into a set of volumes and flows for the FV water quality model that is mass conserving up to machine accuracy. Furthermore, it is shown that this approach works for all hydrodynamic models that solve the continuity equation with the classical finite element method with nodal polynomial base and test functions that need not be equal. In Section 3 the results of a testcase are presented.

2. MASS AND ADVECTION MATRIX IN FEM

The advection–diffusion equation (1) is the transport equation for the concentration C of substances in the water, subject to the diffusion tensor D and the advection vector u:

$$\frac{\partial C}{\partial t} = \nabla \cdot (D \times \nabla C) - \nabla \cdot (uC) \tag{1}$$

This equation is supplemented with Dirac-δ functions for point loads and continuous functions for diffuse sources of the substances. Mutual reaction terms between the different substances in the water will complete the equation to a full water quality model [2]. Here we will limit ourselves to the advection part:

$$\int_{t^n}^{t^{n+1}} \left(\frac{\partial C}{\partial t} + \nabla \cdot (uC) \right) \mathrm{d}t = 0 \tag{2}$$

To maintain consistency, Equation (2) should hold also for water (with concentration 1.0 always and everywhere). This leads in three dimensions to $\nabla u = 0$ and to $\partial h / \partial t = -\nabla h \overline{u}$ for the depth-integrated version of (2). This is the continuity equation of incompressible hydrodynamic flows. The representation of this continuity equation in finite element models results from the multiplication of the equation with sufficiently smooth test functions ψ_i [3]. The finite element form of the depth-integrated continuity equation then becomes (3) [4]. This form has 2 parts: (a) the part of the change in water level or change in mass and (b) the part of the advection or flow:

$$\int_{t^n}^{t^{n+1}} \left(\int_{\Omega} \left(\frac{\partial h}{\partial t} + \nabla \cdot (h\overline{u}) \right) \psi_i \, \mathrm{d}\Omega \right) \mathrm{d}t = 0 \quad \forall i \tag{3}$$

Test functions are either derived per element E and per node as nodal polynomial base or only per element as hierarchical polynomial base [3]. We will limit ourselves to nodal bases. A test function corresponding to node i is 1.0 in i and 0.0 in the other nodes. The polynomial base of element E is expanded to the complete model domain Ω through composition of shape functions around the nodes i from the element base. In this way a set of equations, one per node, results [5]. For node i it contains the addition of all element contributions of the elements sharing node i. The velocity vector u generally comes from the hydrodynamic parts of the set of equations. It may be indirectly influenced by the concentration C (e.g. if C influences water density like for salt, heat and silt). We will elaborate more on both parts of the continuity equation in next sections.

DOI: 10.1002/fld

2.1. The mass matrix in the continuity equation

We assume that depth h is approximated with base functions that equal the test functions according to (4), but application of this Galerkin technique [6] will not be critical for the conclusions. The part of the time derivative of h in (3) then transforms into (5) for an element containing nodes i, j and k. M_E is the mass matrix of element E:

$$\tilde{h} = \sum_i h_i \psi_i \tag{4}$$

$$\frac{\partial}{\partial t} \sum_i \sum_j \int_\Omega h_i \psi_i \psi_j \, \mathrm{d}\Omega = \frac{\partial}{\partial t} M_E \begin{pmatrix} h_i \\ \vdots \\ h_k \end{pmatrix}, \quad i, j, k \in E \tag{5}$$

For triangular elements E with surface area S and linear polynomial base spanned by the 3 vertices, the element mass matrix is easily derived by analytical integration. It is given in (6). The mass matrix consists of $\frac{1}{3}$ of the surface area S of the triangle E times a weighing matrix with rows that sum to 1.0 and terms that indicate the weight of the contribution of the different depth values h in element E to the corresponding node

$$M_E = \frac{S}{3} \begin{pmatrix} 0.50 & 0.25 & 0.25 \\ 0.25 & 0.50 & 0.25 \\ 0.25 & 0.25 & 0.50 \end{pmatrix} \tag{6}$$

The total mass matrix M of the whole model area consists of the sum of all contributions of the element mass matrices. The value of $\frac{1}{3}$ of the surface area of the triangle E can be interpreted as the share of the surface area of E that is attributed to each of its nodes. The finite volume analogue of this FEM consists of centring the finite volumes on the nodes. The horizontal surface area of the finite volume is the sum of $\frac{1}{3}$ of the surface areas of each triangular element E that shares the node. Graphical representation of this area is done by using the lower parts of the gravity lines of the triangles (Figure 1(b)). If both the base functions and test functions sum to 1.0 everywhere, all terms in the mass matrix of an element will sum to the surface area of that element. This follows from the nature of the mass matrix ($\int \varphi_i \psi_j$). Base and test functions need not be the same for this property. The sum of the terms in each row can always be seen as the share of the surface area of E that is attributed to the node of that row. The terms in the matrix row can always be seen

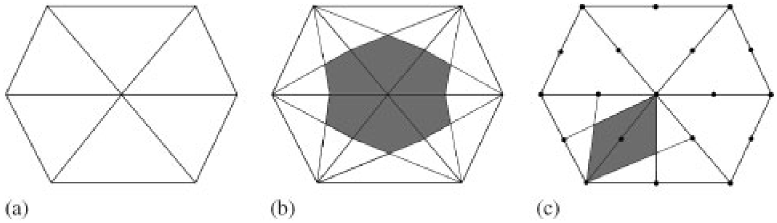

Figure 1. (a) Six triangular finite elements; (b) finite volume around a vertex with linear base; and (c) finite volume around an edge with quadratic base.

DOI: 10.1002/fld

as the weighing factors that are needed to obtain the weighed average finite volume depth of the node of that row, that corresponds to the finite element depth of the nodes.

The mass matrix can be approximated using a diagonal matrix. The diagonal term of a row then consists of the sum of all terms of that row in the exact mass matrix. This procedure is called 'mass-lumping' [3]. If the finite element model uses mass lumping, then there is only one weighing factor located on the diagonal. It consists of the horizontal surface area around the node. In that case the finite volume depth directly equals the finite element depth. Several authors [7, 8] assume mass lumping for an analogue between finite elements and finite volumes. This assumption is however no requirement. The weighing can also be performed *a posteriori* to derive finite volume depths from the non-lumped finite element depths.

This means that for each nodal polynomial base, such a finite volume analogue of the mass matrix exists. It may have remarkable properties for some sets of base and test functions. Examples for triangular elements with 6 nodes and quadratic polynomial base and test functions the mass matrix looks like (7). The uneven rows are the nodes at the vertices and the even rows are the nodes of the midpoints of the edges.

$$M_E = \frac{S}{3}\frac{1}{180}\begin{pmatrix} 18 & 0 & -3 & -12 & -3 & 0 \\ 0 & 80 & 0 & 56 & -12 & 56 \\ -3 & 0 & 18 & 0 & -3 & -12 \\ -12 & 56 & 0 & 80 & 0 & 56 \\ -3 & -12 & -3 & 0 & 18 & 0 \\ 0 & 56 & -12 & 56 & 0 & 80 \end{pmatrix} \tag{7}$$

If mass-lumping is performed, the rows of the nodes at the vertices sum to zero and the rows of the nodes at the midpoints of the edges sum to S/3. This means that then no mass is stored at the vertices and all mass is stored around the edges. Figure 1(c) gives the graphical representation of the finite volume analogue of this combination of elements and polynomial base. The nodes and base functions of the vertices serve to make the polynomial base continuous throughout the model area, but do not store mass if mass is lumped.

The finite element method interpolates the state variables over its elements using the base functions. Linear base functions in Figure 1(b) and quadratic base functions in Figure 1(c). It integrates the equation times the test functions as a weighing. Such integration resembles the integration of the equation itself over the finite volume areas as conducted in the FVM. It yields at least matrix terms with the same dimension. The FEM integration is however different in the sense that the FEM integration is weighed. It furthermore covers the whole area of the triangles that share a certain node. So in the FEM the area of integration for two adjacent nodes overlaps because their base and test functions overlap. This is different from the FVM. The FEM integral results in a horizontal surface area times a weighed average of the water depth h because all nodal polynomial test and base functions sum to 1.0. The piecewise continuous integration of the interpolated water levels h over the finite volume areas of Figures 1(b) and (c) gives however different results because the weighing is lacking and the domain of integration is different. So integration of the interpolated h will not lead to a finite volume analogue of the finite element method [9].

DOI: 10.1002/fld

2.2. *The advection vector in the continuity equation*

The divergence terms of (3) for all nodes k are given by Equation (8). The boundary term vanishes per internal node k because all test functions ψ that correspond with internal nodes k vanish at the boundary of the model domain. The boundary term does not vanish for open boundary nodes, where it represents the flux across the open boundary of the model:

$$\int_{\Omega} \nabla h\bar{u}\psi_k \,\mathrm{d}\Omega = \oint_{\Gamma} h\bar{u}\cdot\bar{n}\psi_k \,\mathrm{d}\Gamma - \int_{\Omega} h\bar{u}\nabla\psi_k \,\mathrm{d}\Omega = -\int_{\Omega} h\bar{u}\nabla\psi_k \,\mathrm{d}\Omega \quad \forall k \notin \Gamma \tag{8}$$

It is common to split up the resulting integral of (8) in integrals per element to evaluate the element contribution to the matrix equation. Per element E the boundary term does not vanish. For each element, the boundary term can be seen as a flux from this element to the adjacent elements, sharing the corresponding edge. For a nodal polynomial base, the test function for a node is continuous on the edges thus the associated internal boundary term leaving one element across an edge enters the adjacent element through the same edge and no mass is lost or gained at the element interfaces. This is the reason why the internal boundary terms need not be evaluated for the element contributions of elements not containing boundary nodes.

If an element E contains n nodes, then an element contribution consists of an integral over the element E as in (8) for each of those n nodes in the system matrix. These n integrals on the n rows for each node sum to zero per element E as shown below:

$$\sum_{k\in E} \psi_k = 1.0 \rightarrow \sum_{k\in E} \int_E h\bar{u}\nabla\psi_k \,\mathrm{d}E = \int_E h\bar{u} \sum_{k\in E} \nabla\psi_k \mathrm{d}E = 0 \tag{9}$$

Equation (9) holds for all sets of nodal polynomial test functions, irrespective of the selected base functions for u. What (9) says is that the flow entering or leaving a single node in this element E equals the sum of the flows leaving or entering the other nodes. So no mass is gained or lost within element E.

In this way all element contributions to node k consist of the flow in that element towards or from node k, depending on the sign. The combination of the mass matrix terms on row k and these flux terms on row k means that the change in mass for node k equals the sum of the fluxes towards node k from all elements E sharing node k. This also means that mass is conserved per node.

It is interesting to take a closer look at $\nabla\psi_k$. For triangular elements with both linear base and test functions defined at the vertices it is a vector with magnitude $1/h_k$ where h_k is the distance of node k to the opposite edge in triangle E (Figure 2(a)). The vector is perpendicular to this opposite edge in the plane of E. The surface area of the triangle S_E is $0.5h_k l_k$ where l_k is the length of the opposite edge. So $\nabla\psi_k$ is a vector with magnitude $0.5l_k/S_E$. This means that the integral (10) for one node in E stands for the average value of hu over element E in the direction normal to edge l_k multiplied with half the length of this edge l_k:

$$-\int_E h\bar{u}\nabla\psi_k \,\mathrm{d}E = -\frac{l_k}{2}\frac{1}{S_E}\int_E h\bar{u}\,\bar{n}_{l_k} \,\mathrm{d}E \tag{10}$$

If the test functions are nonlinear, their derivatives are not constant over E and the integral in (10) becomes a weighed integral with the derivative of the test function as the weighing, but the principle is the same. Figure 2(b) gives a graphical representation of this flux. The line $0.5l_k$ is as long as the projection of the parts of the gravity lines that connect the centre of gravity with the

DOI: 10.1002/fld

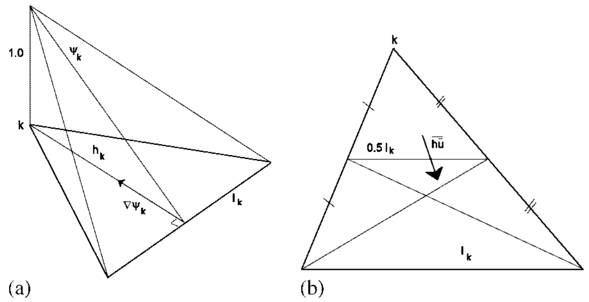

Figure 2. (a) Graphical representation of $\nabla\psi_k$; and (b) $\overline{h\overline{u}}$ through line $0.5 * l_k$.

edges in the direction of l_k. So the physical interpretation is now complete. The fluxes can be seen as the element averaged value of *hu* through the lower parts of the gravity lines in the direction perpendicular to the opposite edges.

This geometrical reasoning also shows in formula. Equation (11) results for the element contribution of E. A_E is the advection vector of E and transforms into (12), with M_E as the mass matrix (see Equations (5) and (6)) of E. With $\tilde{h}$ as $M_E h$, expression (13) results for the flux contributions of the 3 nodes of E to the continuity equation. l_i is the length of the edge opposite to node i and $\overline{n}_{l_i}$ is the unit vector normal to this edge:

$$-\int_E h\overline{u}\nabla\psi_k\,\mathrm{d}E = -\sum_{i,j\in E}\int_E h_i u_j \psi_i \psi_j \nabla\psi_k\,\mathrm{d}E = A_E \quad \forall k\in E \tag{11}$$

$$A_E = -\sum_{i,j\in E} h_i \overline{u}_j \nabla\psi_k \int_E \psi_i\psi_j\,\mathrm{d}E = -\left\{(\overline{u}_i,\overline{u}_j,\overline{u}_k)M_E\begin{pmatrix}h_i\\ h_j\\ h_k\end{pmatrix}\right\}\begin{pmatrix}\nabla\psi_i\\ \nabla\psi_j\\ \nabla\psi_k\end{pmatrix} \tag{12}$$

$$A_E = -\frac{1}{3}S_E(\tilde{h}_i\overline{u}_i + \tilde{h}_j\overline{u}_j + \tilde{h}_k\overline{u}_k)\frac{1}{2S_E}\begin{pmatrix}l_i\overline{n}_{l_i}\\ l_j\overline{n}_{l_j}\\ l_k\overline{n}_{l_k}\end{pmatrix} = -\overline{h\overline{u}}\frac{1}{2}\begin{pmatrix}l_i\overline{n}_{l_i}\\ l_j\overline{n}_{l_j}\\ l_k\overline{n}_{l_k}\end{pmatrix} \tag{13}$$

Up to now nothing has been said about the time level of vectors *hu* in Equations (8)–(13). That is not so important. If, e.g. θ is the share of the implicit part and $(1-\theta)$ is the share of the explicit part, then the vectors *hu* mentioned in the equations stand for the weighed average of the implicit and the explicit part, as they appear in the FEM equations.

2.3. Boundary conditions

Now it is time to deal with boundary nodes and elements that share boundary nodes. Closed boundaries are simplest. We just add the element contributions (5) of all wet elements sharing one or more closed boundary nodes to the total mass matrix M. This gives a change in volume of these boundary nodes that is equal to $\frac{1}{3}$ of the surface areas of all wet elements sharing this node, times the weighed water depths of the nodes of these wet elements. The advection vector

DOI: 10.1002/fld

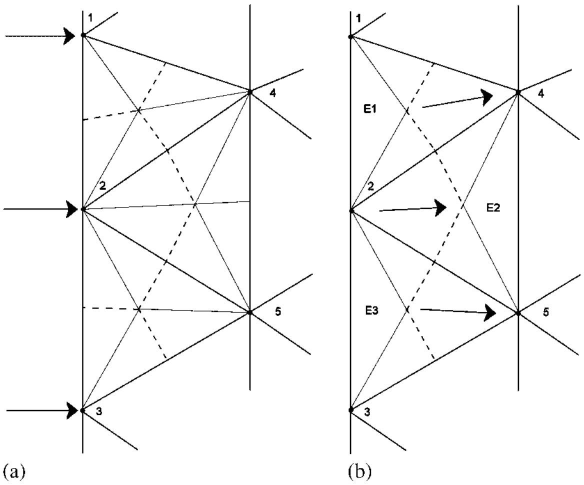

Figure 3. Open boundary nodes 1, 2, 3. Internal nodes 4, 5 and elements E1, E2 and E3.

of the wet triangles sharing this node gives the flows that are leaving and entering the node to and from the other nodes of the wet triangles. The implicit assumption in this approach is that the flow through the boundary edges is zero.

For open boundary conditions the situation is somewhat more complicated. Then the open boundary part of (8) does not vanish. One can distinguish velocity boundaries, water level boundaries and mixed boundaries. It is possible to deal with a velocity open boundary node just as with a closed boundary node, except for an open boundary flux towards this node (Figure 3(a)). That flux consists of all terms of the boundary integral in (8) that are associated with the test function of that node. The changes in water level for that node can then be computed as the result of the fluxes across the open boundary part of that node and the fluxes within the triangles sharing the node. For the water level open boundary the flux entering the open boundary node from the outside generally is not computed and no mass conservation exists for the boundary node itself since it is not part of the interior of the model. To overcome distinction in the kind of open boundaries, we assume that all the open boundary nodes are not part of the model. We assume that the element contributions of all elements sharing a boundary node, towards the first line of internal nodes, exist. The open boundary condition then always acts as a flux boundary between the boundary nodes and the first line of internal nodes. In Figure 3(b) this is illustrated for the boundary nodes 1, 2 and 3 and the internal nodes 4 and 5. The dashed lines give the boundary between the finite volume analogue and the open boundary nodes. The arrows towards node 4 in element E1, from node 2 in element E2 and towards node 5 in element E3 are computed according to (13) and give together the open boundary fluxes in this section of the open boundary.

2.4. Degree of freedom to complete the finite volume analogue

We have derived a set of finite volumes with horizontal surface areas completely covering the internal FEM model area with computational cells around the FEM nodes. We are either using FEM lumped water levels or an equivalent weighing procedure on non-lumped FEM water levels to obtain volumes and changes in volumes around the FEM nodes. We also have derived a set of

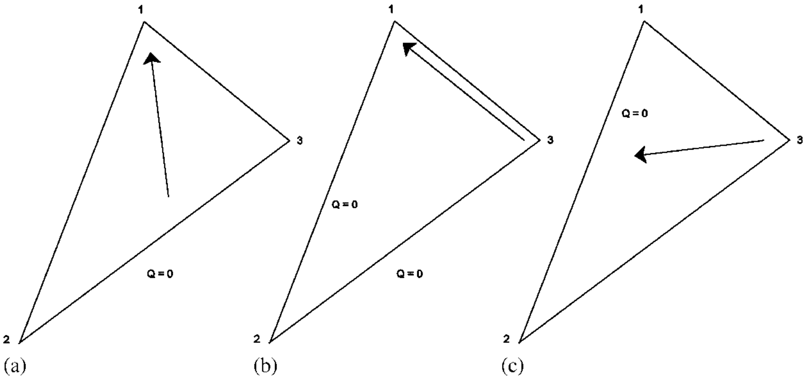

Figure 4. Fluxes that become zero with the 'nearest projection' method.

flux terms to and from the nodes with the property that no flux is lost between the nodes. We can set up the matrix equation in a finite volume way to link the change in water levels in nodes with the fluxes to and from those nodes. We then exactly reproduce, term by term, the matrix equation that is used by the finite element model to describe the same change in water levels for all its internal nodes. In the mean time we have shown that this procedure is fully mass conserving per node for each nodal polynomial base. It seems that we now can conclude that our finite volume analogue of the finite element generated flow field and water levels is ready.

This conclusion is not fully true. Equation (13) gives for an element E the 3 fluxes to and from the 3 nodes in that element. It is mass conserving because the 3 fluxes sum to zero. What we need however are the fluxes *between* the nodes. We know what flux leaves node i, but we do not know yet how much of it goes to j and how much to k. We cannot solve the fluxes between the nodes from those to and from a certain node because for a triangular element there are 3 unknowns and the three knowns are mutually dependent because they sum to zero. So one degree of freedom is left.

There are several strategies to solve this problem. We could expand the analogue and see how the finite element method solves its transport of substance equation. By careful selections of flows and weighed average values of the concentrations in the nodes, we could probably reproduce that set of equations also term by term by the finite volume analogue. That however has little use, because then we could equally well just use the finite element model to solve our water quality model equations. We could also use the geometric reasoning of Figure 2 and split the flows, e.g. according to the length of the projections of the gravity lines.

We followed a different way. Equation (13) shows that for each element a weighed average flow value is used that is projected in the directions perpendicular to the test functions. If we take the direction of this weighed average flow, so the direction of $(\tilde{h}_i\overline{u}_i + \tilde{h}_j\overline{u}_j + \tilde{h}_k\overline{u}_k)$, then it will always be possible to let this direction point towards or from one of the nodes from or towards the interior of triangle E (Node 1 in Figure 4(a), node 3 in Figure 4(c)). We then direct the flow towards or from this node from or towards the two other nodes and we assume zero flow between the two other nodes. Only if the direction coincides with the direction of one of the edges of E, the flow can run exactly between the two nodes spanning the edge and the two other flows are zero (Figure 4(b)). You can call this method a 'nearest projection' method, because the flow along the edge that is closest to perpendicularity with the direction of the flow becomes zero. You can also

DOI: 10.1002/fld

call it a 'zero rotation' method because the rotation of the flow within element E, as a consequence of the attribution to the 3 links between the nodes, becomes zero this way.

2.5. *The analogue in three dimensions*

The analogue in three dimensions depends on the treatment of the water free surface. If there are layers with fixed water level during a time step, then $\nabla u = 0$ for those layers and for incompressible fluid. The 'change in mass part' of (3) then is zero because h does not change. The mass matrix itself however is not zero and still shows the amount of mass that is attributed to each of the nodes. Everything that is mentioned on the advection vector still remains the same, the only difference is that all terms associated with one node sum to zero, because its volume does not change. For those layers where also a change in water depth is computed, the same reasoning as for the depth integrated case holds. It is clear from the concentration of mass in the nodes that a layered finite element model with $n+1$ nodal layers (one at the bottom and one at the water surface) becomes a finite volume model that also has $n+1$ layers. In such models, like in Telemac-3D, the vertical velocities are computed to readjust the layers to their fixed level or to their proportional sigma level. The same procedure can then be used for the analogue to derive the vertical fluxes, as is done for the coupling with Telemac-3D.

If the 3D FEM uses completely 3D elements and if the model thus computes the vertical velocities with the finite element method rather than as a consequence of the readjustment of layers, the situation changes somewhat. The mass matrix then shows again what share of the 3D volumes of each element is attributed to each of its nodes. The advection vector again shows the fluxes to and from the nodes. For nodal polynomial bases the advection terms per element still sum to zero. All according to the given principle and formulas. This however leaves a number of degrees of freedom for the finite volume analogue that is larger now. There are more links between nodes than nodes in the element. For a standing prism with 6 nodes, e.g. there are 6 flows in the advection matrix one towards or from each of the nodes. All 6 together sum to zero. But there are 15 possible finite volume links between the nodes, so there are 10 degrees of freedom. If we assume vertical flows along the edges only, 6 degrees of freedom vanish (are zero). If we also assume that the 3 vertical fluxes in one element are equal, 2 more vanish. If we furthermore use the 'nearest projection method' for both the top triangle and the bottom triangle, then all degrees of freedom are resolved.

The guiding principle again is that the finite volume analogue derived this way produces a matrix equation for continuity that is an exact match of the corresponding finite element matrix equation for continuity, term-by-term.

3. TEST CASES

The test-case was taken in the Telemac-2D validation document [4]. The initial purpose was to study the impact of a channel flow around obstacles and to demonstrate that the software can simulate flows with unsteady eddies even with steady-state boundary conditions. As the finite element mesh used has the same symmetry as the real domain, von Karman eddies will appear only if there is a breaking of symmetry in the computation. This is achieved either by the linear systems solvers, or by truncation errors. A 20 m wide and 28.5 m long prismatic channel with trapezoidal cross-section contains bridge-like obstacles in one cross-section made of two abutments

DOI: 10.1002/fld

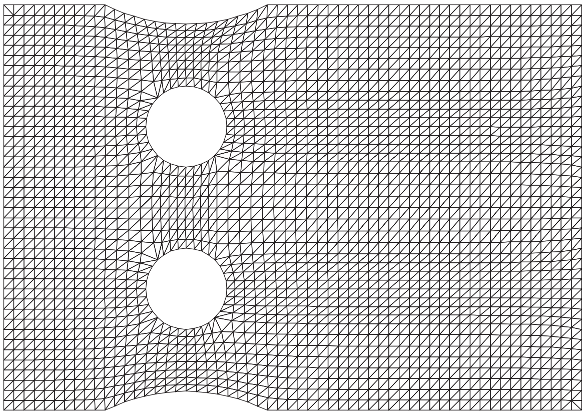

Figure 5. The finite element computational grid of the channel flown from left to right.

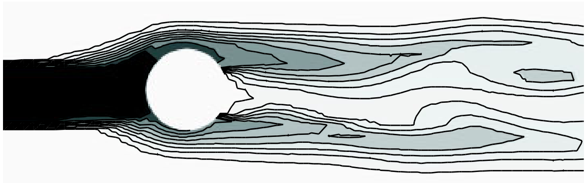

Figure 6. Concentration pattern of the tracer after 400 times steps of 0.1 s with the FEM.

and two circular 4 m diameter piles. There are 4304 triangular elements and 2280 nodes in the mesh (Figure 5). The inflowing open boundary is at the left side, the outflowing open boundary is at the right side. Top and bottom boundaries and also the boundaries along the two pillars are closed.

The elevation of the free surface is imposed at the exit at the value 0. The velocity profile at the entrance is assumed constant and the value of the velocity is recomputed at every time step to ensure that the total discharge is $Q = 62\,\mathrm{m}^3/\mathrm{s}$, whatever the free surface elevation. On the lateral boundaries and pillars, a free slip condition is assumed. The flow resulting from steady-state boundary conditions is studied. The bed is flat in the middle of the channel, at an elevation of -4 m, and then rises up to -1 m when it reaches lateral boundaries. The Strickler friction law is chosen, with a coefficient 40, which is equivalent to a Manning $\frac{1}{40}$. Turbulence and dispersion are simply represented by a constant kinematic viscosity of $0.005\,\mathrm{m}^2/\mathrm{s}$. With such a value von Karman eddies do appear. With higher values, e.g. a viscosity of $0.1\,\mathrm{m}^2/\mathrm{s}$, symmetry is not broken; 80 s of real time are simulated with time steps of 0.1 s. To avoid spurious oscillations due to the collocation of velocity and depth, a quasi-bubble element has been chosen for velocity. The depth is linear. The advection in the momentum equation is treated with the method of characteristics. For the purpose of this paper a tracer was added in the computation and enters the domain through a small section of the upstream boundary. The transport of the tracer in the FEM model is computed with a Lagrangian solution scheme [10] that minimizes artificial spreading but is not conserving mass. The result of this tracer plume after 40 s is shown in Figure 6.

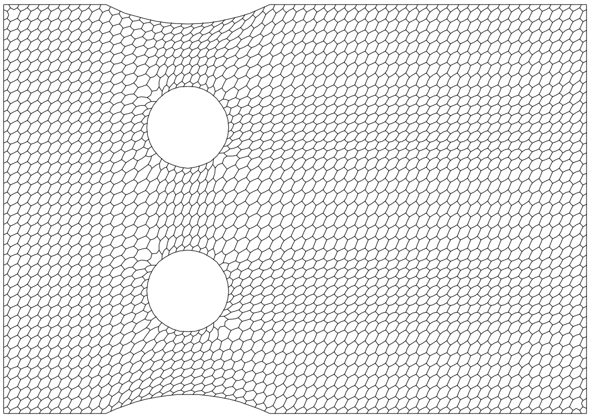

Figure 7. The finite volume computational grid of the channel flown from left to right.

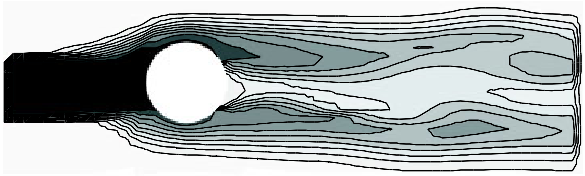

Figure 8. Concentration pattern of the same tracer with the finite volume solver.

The procedure to derive a finite volume analogue of the finite element flow field as described in this contribution is used. The resulting setting of finite volumes is given in Figure 7. The Delft3D finite volume water quality model is used to compute the same tracer release using this finite element model generated flow field. The water quality model now is free to apply its own solvers on the dataset. To demonstrate this, firstly the most simple solver is used: first-order upwind in space, explicit in time. Because of the intrinsic numerical diffusion of the solver, no further diffusion is added. The result is given in Figure 8. The artifact at the inflowing and at the outflowing open boundary is a graphical artifact due to the fact that the open boundary nodes themselves are not part of the interior of the finite volume model.

The results show the same qualitative pattern of tracer transport through the von Karman eddies. The finite volume model conserves mass up to machine accuracy. This is the main reason for the difference in concentration levels more remote from the entrance of the tracer. If the finite volume model uses its more accurate flux corrected transport scheme [11], a diffusion of about $0.0025\,\mathrm{m}^2/\mathrm{s}$ has to be added to obtain comparable results. The principle of the flux corrected transport scheme is in some sense comparable with the SUPG scheme in finite elements: some additional diffusion is added to avoid the wiggles of a higher-order transport solver [12].

Initially the standard output files as produced by the separate Tememac-2D model run have been used to obtain the velocities and water levels in the nodes needed for the computation of flows and volumes. At the moment of the revision of this manuscript the coupling procedure as described has also been implemented as subroutine within Telemac-2D and Telemac-3D to produce the finite volume files directly. This interface also allows for aggregation of time steps to reduce file size. All these interfaces provide sets of volumes and flows between the volumes that are mass conserving up to machine accuracy.

4. CONCLUSIONS AND DISCUSSION

Thanks to a choice of specific finite volumes centred on finite element nodes, a compatibility has been found between finite elements and finite volumes as regards mass conservation and fluxes, so that a finite element hydrodynamics may be used for advection–diffusion type equations solved in finite volumes. The technique developed in two dimensions for shallow water equations can be extended to three-dimensional Navier–Stokes equations with a free surface. This allows a bridge between different software systems working on non structured grids.

The finite volume representation for triangles in two dimensions leaves one degree of freedom. This degree of freedom is used in a way that artificial spreading perpendicular to the direction of the velocity is minimized. The finite volume tracer concentration pattern derived with this flow field even using very simple numerical schemes is similar to the concentration pattern generated with the method of characteristics in the finite element model.

In the basic Telemac-2D algorithm, the continuity equation and the momentum are solved simultaneously. This ensures a strictly coherent depth and velocity as regards continuity. This coherency is converted to a mass conserving finite volume database up to machine accuracy. The method leans on the way the finite element model represents the continuity equation. Another Telemac-2D option exists, based on the wave equation and consisting of eliminating the velocity from the continuity equation [13]. This means that the continuity equation (3) cannot be distinguished in that form any more. This option will also ensure mass conservation, but as the velocity is computed in a further step, it is not compatible with the depth in the sense of Equation (3). This necessitates a different approach to derive a finite volume analogue as will be the case for any other different approach to the continuity equation in finite elements.

REFERENCES

1. Runca E, Bernstein A, Postma L, Di Silvio G. Control of macroalgea blooms in the Lagoon of Venice. *Ocean and Coastal Management* 1996; **30**(2–3):235–257.
2. Chapra SC. *Surface Water Quality Modelling*. McGraw-Hill: New York, 1997.
3. Ern A, Guermond J-L. *Theory and Practice of Finite Elements*. Springer: Berlin, 2004.
4. Hervouet J-M. *Hydrodynamique des écoulements à surface libre*. Ponts et Chaussées, 2003 (English version in press).
5. van Kan J, Segal A, Vermolen F. *Numerical Methods in Scientific Computing*. VSSD: Delft, 2005.
6. Strang G, Fix GJ. *An Analysis of the Finite Element Method*. Prentice-Hall: Englewood Cliffs, NJ, 1973.
7. Idenlsohn SR, Oñate E. Finite volumes and finite elements, two 'good friends'. *International Journal for Numerical Methods in Engineering* 1994; **37**:3323–3341.
8. Neises J, Steinbach I. Finite element integration for the control volume method. *Communications in Numerical Methods in Engineering* 1996; **12**:543–555.
9. Zienkiewicz OC, Oñate E. Finite volumes versus finite elements. Is there really a choice? In *Nonlinear Computations Mechanics. State of the Art*, Wriggers P, Wagner W (eds). Springer: Berlin, 1991; 240–254.
10. Hervouet J-M. Application of the method of characteristics in their weak formulation to solving two-dimensional advection equations on mesh grids. In *Computational Techniques for Fluid Flow*, *Vol. 5. Recent Advances in Numerical Methods in Fluids*, Taylor C, Johnson JA, Smith WR (eds). Pineridge Press: Swansea, 1986; 149–185.

DOI: 10.1002/fld

11. Boris JP, Book DL. Flux corrected transport I. SHASTA, a fluid transport algorithm that works. *Journal of Computational Physics* 1973; **11**:38–69.
12. Brooks AN, Hughes TJR. Streamline upwind Petrov–Galerkin formulations for convection dominated flows with particular emphasis on the Navier–Stokes equations. *Computer Methods in Applied Mechanics and Engineering* 1982; **32**:199–259.
13. Casulli V. Semi-implicit finite difference methods for the two-dimensional shallow water equations. *Journal of Computational Physics* 1990; **86**:56–74.